Biogeosciences Discuss., 9, 7943–7981, 2012
www.biogeosciences-discuss.net/9/7943/2012/
doi:10.5194/bgd-9-7943-2012

Biogeosciences Discussions

Organic carbon and nitrogen export from a tropical dam-impacted floodplain system

R. Zurbrügg[1,2], **S. Suter**[1], **M. F. Lehmann**[3], **B. Wehrli**[1,2], **and D. B. Senn**[1,2]

[1]Institute of Biogeochemistry and Pollutant Dynamics, ETH Zurich, Universitätstrasse 16, 8092 Zurich, Switzerland
[2]Eawag, Swiss Federal Institute of Aquatic Science and Technology, Surface Waters – Research and Management, Seestrasse 79, 6047 Kastanienbaum, Switzerland
[3]Institute of Environmental Geosciences, University of Basel, Bernoullistrasse 30, 4056 Basel, Switzerland

Received: 31 May 2012 – Accepted: 4 June 2012 – Published: 28 June 2012

Correspondence to: R. Zurbrügg (roland.zurbruegg@env.ethz.ch)

Published by Copernicus Publications on behalf of the European Geosciences Union.

Abstract

Tropical floodplains play an important role in organic matter transport, storage, and transformation between headwaters and oceans. However, the fluxes and quality of organic carbon (OC) and organic nitrogen (ON) in tropical river-floodplain systems are not well constrained. We explored the quantity and characteristics of dissolved and particulate organic matter (DOM and POM) in the Kafue River flowing through the Kafue Flats (Zambia). The Kafue Flats are a tropical dam-impacted river-floodplain system in the Zambezi River basin. During the flooding season, >80 % of the Kafue River water passed through the floodplain, mobilizing large quantities of OC and ON, which resulted in a net export of 75 kg OC km^{-2} d^{-1} and 2.9 kg ON km^{-2} d^{-1}, 80 % of which was in the dissolved form. Mass budget estimates showed that ON export, denitrification, and burial caused an annual deficit of ~21 000 t N yr^{-1} in the Kafue Flats. A N isotope balance and the δ^{15}N of DON and PON suggest that N-fixation must level out the large N losses. The elemental C:N ratio of ~20, the δ^{13}C values of higher than –24 ‰, and spectroscopic properties (excitation-emission matrices) showed that DOM in the river was mainly of terrestrial origin. Despite a threefold increase in OC loads due to inputs from the floodplain, the river DOM characteristics remained relatively constant along the sampled 400-km river reach. This suggested that floodplain DOM had similar properties than DOM from the upstream reservoir. In contrast, based on its low δ^{13}C of –29 ‰ and the C:N ratio of ~8, POM originated from phytoplankton production in the upstream reservoir and in the floodplain. While the reservoir had little impact on DOM properties, terrestrial POM was efficiently trapped and, instead, phytoplankton-derived POM was discharged to the downstream Kafue Flats.

1 Introduction

Tropical floodplains are among the most productive and valuable ecosystems worldwide. They can act as major sources or sinks for riverine carbon (C) and nitrogen

BGD
9, 7943–7981, 2012

(N), regulating organic matter (OM) export to downstream systems such as lakes and oceans (Ludwig et al., 1996). Despite the importance of wetlands in the global C cycle, the role floodplains play for riverine C storage, transformation and export has not been well constrained (Battin et al., 2009). This is particularly true for the large wetland areas in the tropics (Bastviken et al., 2010).

A number of studies have investigated the biogeochemistry of dissolved organic carbon (DOC) in different tropical river-floodplain systems (e.g., Alin et al., 2008; Aufdenkampe et al., 2007; Spencer et al., 2010) and identified large differences in age, origin, chemical structure and bioavailability within the DOC pool and between DOC and particulate organic C (POC). While POC has frequently been associated with plant debris, the source allocation of DOC is more complex and often inconclusive (Tremblay and Benner, 2009). The N bound in organic matter (dissolved organic N; DON), however, has seldom been used as a means of DOM characterization in tropical systems (Mladenov et al., 2005), despite DON accounting for 50–90 % of total dissolved N (TDN) and generally high DON exports from tropical catchments (Berman and Bronk, 2003; Wiegner et al., 2009).

The exchange between floodplains and rivers has been identified as a primary factor governing OM mobilization and nutrient dynamics in temperate systems (Hunsinger et al., 2010). In the tropical floodplains of the Amazon basin, river-floodplain exchange has been shown to affect particle distribution and storage (Aalto et al., 2003), cause shifts in the composition of riverine OM due to the injection floodplain-derived OM to rivers (Richey et al., 1990), and foster in-stream mineralization of OM (Mayorga et al., 2005). The emerging number of dams in tropical catchments have the potential to change downstream flooding and thus the hydrological connectivity between rivers and floodplains (Gergel et al., 2005). Dams also efficiently trap particles (Vörösmarty et al., 2003), and both hydrological alteration and particle trapping may affect riverine OM loads and quality in tropical systems (e.g., Bouillon et al., 2009).

To gain better insight into OM dynamics in tropical floodplains and to assess potential dam-impacts OM cycling, we examined the source, quality, and export of OM in the

BGD
9, 7943–7981, 2012

Kafue Flats (Fig. 1a), a floodplain system along the Kafue River, the largest tributary of the Zambezi River. In the Kafue Flats, more than 80 % of the river discharge during the wet season (~600–800 $m^3 s^{-1}$) passes through the highly productive floodplain (Zurbrügg et al., 2012). For comparison, only ~30 % of the river water of the Amazon travels through floodplains (Richey et al., 1989). Intense river-floodplain exchange exerts a strong influence on river biogeochemistry of the Kafue River, as evidenced by pronounced hypoxia over a 150 km long stretch (Zurbrügg et al., 2012). We hypothesized that the backflow from the floodplain carries large OM loads with terrestrial characteristics to the river and would thus affect the riverine OM pool. Additionally, the Kafue Flats system has been impacted by two large dams that have altered the hydrological regime (Zurbrügg et al., 2012), and the flooding patters in the Kafue Flats (Mumba and Thompson, 2005; Meier et al., 2010). We hypothesized that dam operation has changed the characteristics of the OM entering the Kafue Flats and also influenced OM mobilization, transport and quality in the floodplain. The goals of this study were (1) to quantify net export of OC and ON from the floodplain to the river, (2) to determine source, quality and fate of the exported OM, and (3) to explore potential dam impacts on OM characteristics. The stable isotopic composition ($\delta^{13}C$, $\delta^{15}N$) and C:N ratios of DOM and POM were measured to characterize its sources and fate. We also examined spectroscopic properties to identify microbial and terrestrial contributions to DOM (Coble, 1996).

2 Methods

2.1 Study site – Kafue Flats

The Kafue Flats are a 6500-km^2 floodplain system along the Kafue River in Zambia (Fig. 1a). The annual flooding occurs from January to August and is caused by direct precipitation during the rainy season (November–April; mean 800 mm), peak flows of the Kafue River (up to 1900 $m^3 s^{-1}$; Fig. 1b), and seasonal tributaries, creating an

BGD
9, 7943–7981, 2012

extensive wetland area and rich wildlife habitat. The floodplain vegetation fringing the river channel is composed of highly productive C_4-grasses, providing a net primary production of 800–2000 g C m^{-2} yr^{-1} (Ellenbroek, 1987). During the dry season from June–October, river discharge drops to <100 m^3 s^{-1} (Fig. 1b) and the floodplain dries up almost completely. The land use in the immediate catchment is traditional, that is, small scale cattle farming and fisheries, and large areas remain unutilized. Large sugar cane plantations are located along the last 60 river-km, leaving the Kafue Flats a relatively pristine floodplain.

The hydrology of the Kafue River (Q_{avg} ~300 m^3 s^{-1}) has been influenced by two large dams at Itezhi-Tezhi (ITT; closed in 1978) immediately upstream of the Flats, and Kafue Gorge (closed in 1972), immediately downstream of the flats (Fig. 1c). At ITT dam, water is released to the floodplain via spillways, draining the reservoir's epilimnion. A recent study by Kunz et al. (2011) showed that ITT reservoir (with a hydraulic residence time of ~0.7 yr) efficiently traps particles and removes 50 % of N and 60 % of P inputs from the Kafue River.

Intense hydrological exchange between river and floodplain has been identified as a major feature in the Kafue Flats (Zurbrügg et al., 2012). Lateral exchange with the inundated floodplain emerged 220 km downstream of ITT dam, where a channel constriction diverted ~70 % of the stream flow into the floodplain (Fig. 2). The backflow from the floodplain caused a seasonally-recurring steep decline in dissolved oxygen (DO) concentration to <1 mg l^{-1} and low DO levels (<2 mg l^{-1}) along a 150-km reach of the river. Based on natural tracer calculations (specific conductivity and $\delta^{18}O$-H_2O), more than 80 % of the water leaving the system passed through the floodplain (Fig. 2). Changes of timing and extent of ITT dam release have altered the flooded areas in the Kafue Flats (Mumba and Thompson, 2005) and reduced water exchange between river and floodplain by up to 50 % (Zurbrügg et al., 2012).

BGD
9, 7943–7981, 2012

2.2 Sampling campaigns

After a pilot campaign in May 2008, three spatially intensive sampling campaigns were carried out during the dry season (October 2008), and flooding season in May 2009 and May 2010 (Fig. 1b). Sampling was conducted along the Kafue River at ~20 km resolution from downstream of the spillways at ITT dam (0 km) until the end of the floodplain (410 km; Fig. 1c). To characterize floodplain waters, additional samples were taken along 2–7 km transects perpendicular to the Kafue River into the floodplain (T1–T3), and from the wetland boundaries towards the floodplain in Blue Lagoon National Park (T4–T5; Fig. 1c) in May 2010. Water samples were pumped from mid depth in the middle of the well-mixed river channel through polyethylene tubing, using a peristaltic pump (Ejikelkamp, 12 VDC Standard). Samples for DOC and DON, and spectroscopic analyses were filtered in the field through 0.7 µm GF filters (Whatman) into glass bottles and LDPE bottles for DON. Samples for spectroscopic analyses were kept at 4 °C in the dark and analyzed 3–4 weeks after sampling. Water samples for elemental and isotope analyses were acidified to pH 2.5 and frozen until further analysis. For POC and particulate ON (PON) characterization, particles from ~2 l of water were collected on GF filters (0.7 µm/Whatman) and frozen until analysis. All sampling equipment was 2 M HCl/MilliQ-washed, glassware and filters were, in addition, pre-combusted (6 h at 450 °C). For comparative analyses, we also sampled floodplain vegetation and soil, river sediment, and dry deposition (see supplement for details).

2.3 Laboratory analyses

2.3.1 Concentrations and stable isotopic composition of DOC, POC and PON

DOC concentration was measured on a Shimadzu 5050 TOC analyzer. POC and PON concentrations and its C and N isotopic composition (δ^{13}C-POC and δ^{15}N-PON, respectively), were measured on dried (3 h at 40 °C) GF filters. The sediments of ITT reservoir contained only negligible amounts of inorganic carbon (Kunz et al., 2011)

BGD
9, 7943–7981, 2012

and the epilimnion was undersaturated with respect to $CaCO_3$ (data not shown), which made acidification of POM samples redundant. Filter sections were enclosed in tin capsules and measured on a FlashEA 1112 coupled to a DeltaV Adantage Continuous-Flow Isotope Ratio Mass Spectrometer (FlashEA-CF-IRMS; ThermoFinnigan). In-house EDTA ($\delta^{13}C = -30.25‰_{VPDB}$; $\delta^{15}N = -1.1‰_{air}$) and ammonium oxalate ($\delta^{13}C = -17.02‰_{VPDB}$; $\delta^{15}N = +32.7‰_{air}$) were used as standards, with a precision of $\pm 0.1‰_{VPDB}$ for $\delta^{13}C$ and $\pm 0.2‰_{air}$ for $\delta^{15}N$. The isotopic ratios are reported using the delta notation, that is, $\delta^{13}C$ or $\delta^{15}N = (R_{sample} - 1) \times R_{standard} \times 1000‰$, where R is the isotopic ratio (^{13}C:^{12}C or ^{15}N:^{14}N) of the sample (R_{sample}) and the standards ($R_{standard}$), which are Vienna Pee Dee Belemnite (VPDB) for C and atmospheric N_2 for N.

For the C-isotope analysis of DOC (δ^{13}C-DOC), 1 ml of 5 g l^{-1} high-purity, precombusted K_2SO_4 was added to 40 ml of sample and the acidic samples were purged for 2 min with Ar to remove inorganic C (HCl had been added after sampling in the field), refrozen and freeze-dried (Schwendenmann and Veldkamp, 2005). The precipitate was measured on the same FlashEA-CF-IRMS using IAEA-CH6 sucrose ($\delta^{13}C = -10.45‰_{VPDB}$), EDTA and ammonium oxalate as standards at an analytical precision of $\pm 0.1‰_{VPDB}$. The analytical precision is based on replicate measurements of untreated standards of sucrose ($n = 7$) and ammonium oxalate ($n = 7$) of and standards that were processed as samples ($n = 6$ and $n = 8$), respectively.

2.3.2 Concentrations of DIN and DON, and δ^{15}N-TDN

For dissolved inorganic N (DIN), NH_4^+ and NO_2^- were measured using standard colorimetric techniques. The sum of NO_3^- and NO_2^- was determined by reduction to NO_x (Braman and Hendrix, 1989) in an acidic vanadium (III) solution in an Antek 745 preparation module followed by chemoluminescence detection (Antek 9000), and NO_3^- was calculated by difference.

TDN was measured according to Solorzano and Sharp (1980) and Bronk et al. (2000) by oxidizing 12 ml of filtered sample to NO_3^- with 2 ml of persulfate oxidizing

BGD
9, 7943–7981, 2012

reagent (POR), which consisted of 6 g potassium peroxidisulfate ($K_2S_2O_8$) and 6 g NaOH (both ACS-grade) per 100 ml MilliQ water (Knapp et al., 2005). In order to reduce the nitrogen blank of POR, the peroxidisulfate salt was recrystallized 3–5 times according to Grasshoff et al. (1999) and stored under Ar atmosphere. Samples with POR were autoclaved in 30 ml Pyrex vials (acid washed, precombusted, PTFE-lined lids) for 55 min and NO_3^- concentration was measured as described above. IAEA-N2 (+20.3 ‰$_{air}$), USGS-41 (+47.6 ‰$_{air}$), urea (+0.24 ‰$_{air}$), and EDTA were used as processing and isotopic standards, and were oxidized with the samples over the expected concentration range (Fig. S1, supplement). The oxidation yield was 95–106 % after blank correction. Duplicates of pure POR solution were oxidized with every run to determine the contribution of POR to the N blank. The POR blank contribution was generally 0.5 ± 0.3 µM per sample which is equal to ∼3 % of the sample TDN. DON concentrations were calculated as $DON = TDN - NO_3^- - NO_2^- - NH_4^+$.

The $\delta^{15}N$ ratio of TDN-derived NO_3^- ($\delta^{15}N$-TDN) was measured according to Knapp et al. (2005) and Bourbonnais et al. (2009), combining persulfate oxidation and the denitrifier method (Casciotti et al., 2002; Sigman et al., 2001) where NO_3^- is bacterially converted to N_2O. After microbial reduction of NO_3^-, N_2O was measured on a modified GasBench II with a GC PAL autosampler coupled to a Delta Plus XP Continuous Flow IRMS (all instruments ThermoFinnigan). IAEA-NO_3 (+4.7 ‰$_{air}$) and in-house UBN1 (+14.2 ‰$_{air}$) were used as $\delta^{15}N$-NO_3^- standards. DON dominated TDN in all samples (generally >94 %), therefore, $\delta^{15}N$-TDN can be considered a reasonable approximation to $\delta^{15}N$-DON.

2.3.3 Spectroscopic analyses

The spectroscopic analyses consisted of UV absorbance spectroscopy and fluorescence spectroscopy. To constrain the source and chemical character of DOM we measured specific UV absorption at 254 nm ($SUVA_{254}$), which is a measure of the aromaticity of the DOM (Weishaar et al., 2003). UV absorption from 200–700 nm was measured

BGD
9, 7943–7981, 2012

in a 1 cm quartz cuvette using a UV-VIS spectrophotometer (Varian Cary 100Bio) and $SUVA_{254}$ was calculated as

$$SUVA_{254} = \frac{Abs_{254}}{[DOC]} \left[l\,mg^{-1}\,m^{-1} \right] \quad (1)$$

whereby Abs_{254} is the absorption measured at 254 nm and [DOC] is the DOC concentration.

Excitation-emission matrixes (EEMs; Coble, 1996; McKnight et al., 2001) were obtained for each of the 45 filtered whole water samples from May 2010 over an excitation range from 240 to 450 nm in 5 nm increments an emission range from 320 to 550 nm in 2 nm increments on a Fluoromax-4 spectrofluorometer (Horiba Jobin Yvon). All matrices were corrected for the inner-filter effect, using measured UV absorbance (Lakowicz, 2006), for lamp decay (Stedmon et al., 2003), and normalized for the Raman area. Parallel factor analysis (PARAFAC) was used to identify underlying fluorescence components following the procedures of Stedmon et al. (2003) and Stedmon and Bro (2008). A series of PARAFAC models with two to eight components were fitted to the data and we found that a four-component model gave the best representation of the EEMs' fluorescence signal. Details on PARAFAC modeling are given in the supplement section. In order to distinguish between terrestrial and microbial (i.e., algal/bacterial) origin of DOM, the fluorescence index (FI; Cory et al., 2010) was calculated as

$$FI = \frac{Em_{470}}{Em_{520}} \quad (2)$$

Em_{470} and Em_{520} are the emission intensities at wavelengths of 470 nm and 520 nm, respectively, at an excitation wavelength of 370 nm. FI values of >1.4 indicate microbial and <1.4 primarily terrestrial origin (Cory et al., 2010).

BGD
9, 7943–7981, 2012

2.4 Statistical analyses

Correlations between normally-distributed parameters were determined by linear regression, and by Spearman's correlations for not normally-distributed data. To evaluate differences between pooled data, we used ANOVA, if normally-distributed, otherwise non-parametric Kruskal-Wallis tests, both at a critical level of 0.05. Averaged data are given as mean ± SD. Statistical analyses were done with SigmaPlot 11.

3 Results

3.1 Organic carbon and nitrogen concentrations along the Kafue River

During both flooding season campaigns in May 2009 and May 2010, DOC concentrations increased from ~250 µM immediately downstream of ITT dam (0 km) to ~400 µM at end of the floodplain (410 km; Fig. 3a). Most of the DOC increase occurred after 230 km, where we have documented that a large influx of floodplain-derived water begins entering the river (Fig. 2). In the dry season (October 2008), DOC concentrations remained relatively constant at 280 ± 50 µM along the entire river reach. DON concentrations showed a similar 2-fold increase, from ~10 µM at the dam site to maximum concentrations of ~20 µM at 410 km in May 2009 and May 2010. In October 2008, DON was found at fairly constant concentrations of 14 ± 1.2 µM. For all three campaigns, ON was the dominant form of N, representing 93–97 % of total N while DIN, mainly in form of NO_3^- and NH_4^+, was generally <1.5 µM (data not shown). DOC concentrations in the inundated floodplain (May 2010) tended to be higher than in the adjacent river station, reaching up to 600 µM (Fig. 3a). Floodplain DON concentrations were comparable to those measured in the Kafue River.

During the flooding season, concentrations of POC and PON were ~40 µM and ~6 µM, respectively, after ITT dam (Fig. 3b) and decreased by a factor of 2–3 between 200 km and the end of the Kafue Flats. POC and PON concentrations measured in

BGD
9, 7943–7981, 2012

May 2009 increased slightly over the first 70 km. In October 2008, the concentrations of both parameters were comparable to values observed during flooding, but pronounced peaks in POC and PON were detected between 200 and 300 km, which are consistent with higher particle concentrations along this stretch (Fig. S2a, supplement).

The molar ratio of DOC:DON remained relatively constant along the river during flooding season sampling campaigns, with values of 19.7 ± 2.4 in May 2010 and 23.2 ± 2.3 in May 2009, respectively (Fig. 3a). In general, DOC:DON was similar (mean 19.3) in October 2008, with the exception of some lower values between 200–300 km. Across all three sampling campaigns, POC:PON (7.9 ± 0.9 in May 2010; 8.6 ± 0.7 in May 2009; 10.7 ± 1.9 in October 2008) was 2–3 fold lower than DOC:DON (Fig. 3b).

3.2 Carbon and nitrogen stable isotopes

Values for δ^{13}C-DOC in the river were confined to a fairly narrow range (–21.0 ‰ to –24.7 ‰) for all three sampling campaigns (Fig. 4). Nonetheless, some systematic variations were evident. During the May 2010 campaign, δ^{13}C-DOC exhibited a distinct increase from –23.9 ‰ to –21.7 ‰ over the first 90 km, and during both flooding season campaigns δ^{13}C-DOC decreased by 2.5 ‰ after 250 km. Along the floodplain transects, high δ^{13}C-DOC tended to co-occur with high DOC concentrations, mostly in the more distant sections from the river channel. During the dry season, δ^{13}C-DOC did not show systematic variation along the river channel. Across all sampling campaigns, POC at river stations was systematically depleted in ^{13}C relative to the corresponding DOC (mean difference = 5.1 ± 1.7 ‰; Fig. 4). During the flooding season, δ^{13}C-POC increased by 2.5 ‰ over the first 100 km downstream of ITT dam. The δ^{13}C-POC of floodplain samples varied substantially, covering a range of –33.7 ‰ to –23.4 ‰. During the dry season, δ^{13}C-POC along the river was again relatively constant at –26 ‰.

δ^{15}N-TDN values during the May 2010 and May 2009 campaigns exhibited limited variability along the river (2.1 ± 0.4 ‰ and 1.4 ± 0.5 ‰, respectively; Fig. 4). On average, δ^{15}N-TDN was similar in October 2008, but had somewhat greater variability (2.5 ± 0.9 ‰). During the flooding season campaigns, δ^{15}N-PON immediately

BGD
9, 7943–7981, 2012

downstream of the ITT dam was ~2 ‰ higher than δ^{15}N-TDN, and gradually decreased to values comparable to δ^{15}N-TDN further downstream (Fig. 4). Floodplain δ^{15}N-PON in May 2010 covered a considerably wider range than observed in river samples (0.3 ‰ to 5.7 ‰).

3.3 Spectroscopic analyses of DOM

$SUVA_{254}$ did not change significantly along the river ($P = 0.077$) but remained at $3.5 \pm 0.3\,l\,mg^{-1}\,m^{-1}$ (Fig. 5a) and was not affected by intensified river-floodplain exchange after 230 km. Floodplain and tributary samples showed smaller but more variable values than the adjacent river reach. Similar to $SUVA_{254}$, FI values along the main channel fell in a very narrow range between 1.42 and 1.47 and exhibited only minor, non-significant ($P = 0.117$) variation along the river (Fig. 5b). The EEMs showed a high degree of similarity among the stations along the river (Fig. 6a) and floodplain transects (Fig. 6b). Two main fluorescence peaks were detected at an excitation/emission wavelength of 345/440 nm, and 240/430 nm (Fig. 6). These peaks are common features in natural DOM and have been named Peak A and Peak C (Coble, 1996), respectively.

4 Discussion

4.1 Net export of organic carbon and nitrogen from the Kafue Flats

The Kafue River's channel morphology is conducive to intense exchange with the floodplain, yet this exchange is highly variable along the river (Fig. 2). Between 180 and 225 km, a large fraction of the stream flow was forced into the floodplain, while downstream of the 300 km mark, water returned from the floodplain into the river, resulting in a ~4-fold increase in discharge (Fig. 2). Thus, most of the discharge of the lower Kafue River in May 2010 and May 2009, as well as its chemical loads, originated in, or passed through, the floodplain. Comparable levels of exchange occurred when

BGD
9, 7943–7981, 2012

flow rates substantially exceeded ~200–300 $m^3 s^{-1}$ (December–July; Zurbrügg et al., 2012). During low-flow periods (August–November), the exchange with the floodplain was substantially reduced.

We combined discharge measurements with concentration data to quantify mass loads of OC and ON along the river (Fig. 7; Table 1). In May 2010, the minimum discharge and minimum DOC and DON loads were observed at ~230 km (Fig. 2) after ~85 % of the flow and loads had been diverted to the floodplain (Fig. 7). Downstream of 230 km, discharge and concentrations of both DOC and DON increased, resulting in a threefold increase in loading (Table1). As DOC and DON mass loads at 410 km were 2.7 and 2.3 times larger than at the dam, and some of the DOC and DON entering the floodplain may have been metabolized before reentering the river, a minimum of 63 % of DOC and 56 % of DON in the river originated from the floodplain. Load patterns in May 2009 for DOC and DON were, overall, similar to those in May 2010, indicating that the large export pulses of DOC and DON from the Kafue Flats are a recurring seasonal phenomenon (Fig. 7). In contrast, during the dry season (October 2008), loads were reduced and remained relatively constant along the river. Loads for POC and PON increased by ~70 % and ~40 % in May 2010 but decreased by 1–2 % in May 2009 and by >40 % during the dry season.

The short travel times of 1.5 weeks along the river (average velocity of ~0.5 $m s^{-1}$ and relatively constant flows for several weeks around the sampling time period (Zurbrügg et al., 2012) allowed for a comparison of upstream and downstream loads. Strictly speaking, our results represent "snapshots" in time, which may not represent the conditions between the annual sampling campaigns, i.e. the bulk of the year. However, results from a bi-monthly sampling campaign that was carried out over one year at several stations along the river indicate, that the net export of OM predominates for several months each year. Over an annual cycle, the net export from the Kafue Flats was ~60 000 t OC yr^{-1} and ~1800 t ON yr^{-1}, respectively (Wamulume et al., 2011).

The maximum flooded area during the 2009/2010 rainy season was estimated 3060 km^2 in March 2010 (F. Köck, personal communication, based on an inundation

BGD
9, 7943–7981, 2012

model described in Meier et al., 2010). The least inundation was recorded in October 2009 (234 km^2). Based on the export estimates for the 2010 and 2009 flooding seasons and the maximum flooded area, the area specific OC (= DOC + POC) yields were 75 $kg\,C\,km^{-2}\,d^{-1}$ for May 2010, and 35 $kg\,C\,km^{-2}\,d^{-1}$ for May 2009 (Table 1). The yields correspond to 1–3 % of the floodplain's annual estimated primary production of 1200 $g\,C\,m^{-2}\,yr^{-1}$ (Ellenbroek, 1987), suggesting that OM burial, mineralization, burning and grazing are more important C-turnover processes in the floodplain. The use of the maximum flooded area may substantially overestimate the flooded area that is in connection with the river, e.g. due to high evaporation in the floodplain (up to 40 %; Zurbrügg et al., 2012) and disconnected water bodies. However, even with a 10 times smaller area, the OC yields would be <30 % of the estimated primary production, which shows that other fates of OM are more important.

The ON (= DON + PON) exports from the Kafue Flats were on the order of 6–9 $t\,N\,d^{-1}$, which corresponds to area normalized yields of 2.9 $kg\,N\,km^{-2}\,d^{-1}$ for May 2010 and 1.9 $kg\,N\,km^{-2}\,d^{-1}$ for May 2009 (Table 1). Compared to model predictions on the scale of the entire Zambezi River basin of 0.14–0.27 $kg\,N\,km^{-2}\,d^{-1}$ for DON (Harrison et al., 2005) and 0.30–0.49 $kg\,N\,km^{-2}\,d^{-1}$ for total ON (Mayorga et al., 2010), the Kafue Flats represent a substantial local source of riverine ON to the Kafue and the Zambezi Rivers, in particular given that these areal rates are likely underestimates based on the use of maximum area. South American tropical catchment DON export rates (0.5–1.0 $kg\,N\,km^{-2}\,d^{-1}$) are also substantially less than those from the Kafue Flats (Mayorga et al., 2010).

4.2 Source of organic matter

Floodplain-derived DOM can in principle originate from three main sources which can have distinct chemical signatures and bioavailability: (1) mobilization from floodplain soils during drainage (aged OM; Mladenov et al., 2005), (2) decaying floodplain vegetation (young OM; Maie et al., 2006), or (3) exudates from phytoplankton, periphyton or microbial biomass (Ziegler and Brisco, 2004). POM could be from relatively

BGD
9, 7943–7981, 2012

fresh plant debris, previously deposited and re-suspended aged POM or eroded soils (Hedges et al., 2000), or phytoplankton and detached periphyton (Wiegner et al., 2009). Significant differences between the C:N ratios of DOM and POM ($P < 0.05$) and between δ^{13}C of DOC and POC across all campaigns indicate that DOM and POM derived from distinctly different sources (Fig. 8). POM had a substantially lower C:N elemental ratio (~8) than DOM and floodplain soils and sediments (Table S1, supplement). The relative elemental N-enrichment (i.e., lower C:N) and ^{13}C-depletion suggest of POM mainly consisted of phytoplankton (Hamilton and Lewis, 1992). This is consistent with the high C content of the suspended particulate material leaving the ITT reservoir (30–40 wt % C), which supports the notion that POM immediately downstream of the dam consisted of the primary production of the reservoir (Fig. S2b, supplement). The consistently high DOC:DON (19–23; Fig. 3a) observed during all sampling campaigns and across all sites indicates an N-poor DOM pool, one that had likely undergone considerable reworking and was probably fairly refractory. Several studies in the Amazon River have documented high DOC:DON in refractory, degraded DOM from lowland reaches of Amazon tributaries (Aufdenkampe et al., 2007), dominated by fulvic and humic substances (Hedges et al., 2000), or soil-derived DOM (Bernardes et al., 2004). In contrast to other systems like the Tana River in Kenya (Bouillon et al., 2007) or the Amazon (Raymond and Bauer, 2001), where δ^{13}C-POC was higher than δ^{13}C-DOC and DOC could originate from POC degradation, this is unlikely in the Kafue Flats, because of the consistently higher δ^{13}C-DOC (Fig. 4).

Spectroscopic results generally support the chemical data that DOM was primarily of terrestrial origin, but also revealed a microbially-derived contribution. The $SUVA_{254}$ values for the Kafue River of ~3.5 l mg^{-1} m^{-1} are characteristic for humic substances of ~25 % aromaticity (Weishaar et al., 2003). Similarly, the two peaks detected in the EEMs, fall in the range of "humic-acid like" DOM (Peak A), and "fulvic acid like" and "hydrophobic acid like" DOM (Peak C), respectively (Chen et al., 2003). The FI of ~1.43, however, indicates both terrestrial (FI < 1.4) and microbial (FI > 1.4) contributions to DOM (Cory et al., 2010). Because of the relative stability of terrestrial DOM, the FI

BGD
9, 7943–7981, 2012

is often negatively correlated with DOC concentration (Johnson et al., 2011; Petrone et al., 2011), but no significant correlation of FI or $SUVA_{254}$ with DOC was found in the Kafue River ($P < 0.05$). FI in other tropical systems ranged from 1.21–1.41 on the Guayana Shield, Venezuela (Yamashita et al., 2010a) and 1.3–3.0 in the lower Amazon basin (Johnson et al., 2011), and in subtropical systems from 1.28–1.47 in the Everglades (Yamashita et al., 2010b) to 2.0–2.3 in the Yangtze River Basin (Chen and Zheng, 2012). The microbial signal in the FI of the Kafue River DOM could be associated with the onset of microbial degradation of mobilized of terrestrial OM after the peak flow (Johnson et al., 2011; Mladenov et al., 2005).

The four components C1-C4 derived from the PARAFAC analysis provided additional evidence for terrestrial DOM with some minor microbial contribution. All components had been identified in previous studies (Fig. S3 and Table S2, supplement) and were found characteristic for humic-like substances (Stedmon and Markager, 2005). The components C1 and C3 are exclusively from terrestrial origin while C2 and C4 can also have microbial origin. A detailed evaluation of components C2–C4 is given in Ishii and Boyer (2012). In summary, DOM in the Kafue River was mainly of terrestrial origin with some microbial contribution while POM had a distinct phytoplankton signature. During the flooding period, the chemical characteristics ($\delta^{13}C$, $\delta^{15}N$, C:N) showed only small variation along the river which is discussed in the next section.

4.3 Dam effects and changes in POM characteristics along the river

In the Kafue River basin, terrestrial POM is efficiently retained in the ITT reservoir upstream of the Kafue Flats, as indicated by intense sediment accumulation (Fig. 9a; Kunz et al., 2011) and the elevated $\delta^{13}C$ and C:N relative to epilimnetic POM (Table S1, supplement). The POM that was released from the reservoir had lower $\delta^{13}C$ and C:N, and likely consisted of phytoplankton from the reservoir's primary production. This injection of authigenic, ^{13}C-depleted POM has also been documented in other systems (Bouillon et al., 2009; Chen and Jia, 2009). In these studies, $\delta^{13}C$-POC rebounded after the dam, similar to our observation from 0–90 km during the flooding

BGD
9, 7943–7981, 2012

season (Fig. 4). However, C:N ratios remained relatively constant along the river, despite the 3 to10-fold increase in POC and PON loads after 300 km (Fig. 7) that requires POM from the floodplain entering the river. The increasing loads and decreasing concentrations suggest that some POM settled out, or was degraded during the floodplain transit, but was replaced by floodplain-derived POM. This additional POM dominated particle loads in the river after 230 km but caused only modest changes in the C:N ratio and the isotopic signatures of riverine POM. We therefore conclude that floodplain-derived POM and reservoir POM have similar characteristics. The floodplain-derived POM could originate from phytoplankton and periphyton from the floodplain, which would explain the low δ^{13}C-POC along some floodplain transects (Fig. 4). Periphyton was found ubiquitous on inundated floodplain vegetation, and open lagoons on the floodplain can be sites of high primary production, even under low nutrient conditions (Cotner et al., 2006).

4.4 Dam effects and changes in DOM characteristics along the river

Given the fresh, reservoir-derived POM entering the Kafue Flats, one would also expect strong evidence for recently-fixed C in the DOM pool, e.g. as DOM released from algae or bacteria or produced during their decomposition. We found that, based on spectroscopic data ($SUVA_{254}$, EEMs and FI), DOM sampled even directly after the dam wall showed a strong terrestrial signal with only minor microbial contribution. In addition, DOM characteristics (C:N, δ^{13}C, δ^{15}N) only moderately shifted with the addition of a large proportion of floodplain-derived DOM. The relatively constant DOM composition suggests that a large fraction of the DOM that exited the reservoir was of terrestrial origin and transited the reservoir basically unchanged (Fig. 9a). Any more bioavailable DOC produced within the reservoir was probably metabolized under the fairly warm in situ conditions (T ~ 20–27 °C). Upstream wetlands that are hydrologically connected to the Kafue River (Lukanga and Busanga Swamps; total area = 4600 km^2) are a potential source of this floodplain-like DOM that had entered the ITT reservoir (Fig. 9a).

BGD
9, 7943–7981, 2012

Results from fluorescence spectroscopy and stable isotope measurements revealed subtle changes in DOM composition along the river transect beginning at ~250 km. The decrease in δ^{13}C-DOC after ~250 km during flood season (Fig. 4), for example, indicates an inflow of DOC with an average δ^{13}C of –30.2 ‰, based on a two end-member mixing calculation. This, in turn, suggests, a relative increase in the abundance isotopically-light DOM, produced from bacteria or algae. Kafue River δ^{13}C-DOC values (–25 ‰ to –21 ‰) were intermediate between δ^{13}C-values for floodplain soil/sediment, and C_3-plant signatures (Table S1, supplement), and do not indicate any significant contribution from vegetation fringing the Kafue River, which is heavily dominated by C_4-plants (Ellenbroek, 1987), with a distinct C isotopic signature of –13 ‰. Grazing, fire or rapid microbial turnover of C_4-derived DOM could explain the absence of a distinct isotopic C_4 signal in δ^{13}C-DOC.

The PARAFAC components showed additional variation in DOM composition along the river. The component's peak fluorescence intensity (F_{max}) sharply increased ($P < 0.001$) between 230 and 280 km for all four components (Fig. S4, supplement). For each component, F_{max} was moderately to strongly correlated with DOC concentration ($R^2 = 0.68 - 0.87$), with C3 ("terrestrial-humic") showing the highest correlation. To detect changes in the DOM fluorescence properties along the river, while correcting for the influence of varying DOC concentrations (Cory and McKnight, 2005; Stedmon et al., 2003), we present the F_{max} ratios of C1, C2 and C4 relative to C3 (Fig. 10). The decrease in terrestrial-humic C1 and the sharp decrease of C2 after 230 km indicate that the chromophoric DOM shifted towards more terrestrial origin as floodplain waters entered the river. Along the floodplain transects, C1 and C4 increased with increasing distance from the river to the floodplain and from the shore to floodplain (Fig. S6, supplement), indicating higher abundance or production, of DOM with C1 and C4-like fluorophores in the floodplain. On the other hand, abundance of C2-like DOM decreased along the river and along the floodplain transects, which suggests that C2 could be related to upstream OM sources and is being diluted by floodplain waters.

BGD
9, 7943–7981, 2012

4.5 Nitrogen balance, DON bioavailability and N-fixation

We combined N loads and stable isotopic signatures to obtain a N balance for the Kafue Flats flooded area over an annual cycle (Fig. 9b). The N fluxes were calculated using own data, literature values from the Kafue Flats, except for denitrification which was approximated using conservative rates from the Amazon floodplains (Kern et al., 1996; Villar et al., 1998). Budget calculations revealed an N deficit of ~21 000 t N yr^{-1} in the Kafue Flats, which is six times higher as the N input from the reservoir and equal to ~57 µmol N m^{-2} h^{-1}. The availability under natural hydrological conditions is unknown, but the construction of the ITT dam in 1978 may have increased the N-deficit. Burial and denitrification in the reservoir remove up to 3900 t N yr^{-1} from the river, which is equivalent to ~50 % of the N inflows in ITT reservoir (Kunz et al., 2011). The annual measured N inflows reservoir from Wamulume et al. (2011) which are indicated in Fig. 9a underestimated the actual loads because of the insufficient sampling resolution during the "first flush" of N at the onset of the rainy season. The revised loads are 7900 t N yr^{-1} based on the model fluxes of Kunz et al. (2011). Nevertheless, dam removal is substantial compared to the N that enters the Kafue Flats through the reservoir (Fig. 9b), a large part of which we identified as refractory DON.

The narrow range of δ^{15}N-TDN (Fig. 4) did not allow to discriminate between floodplain DON and reservoir DON (1.9 ± 0.4 ‰; Table S1, supplement), but supports the paradigm that riverine DON in general originates from terrestrial sources (Berman and Bronk, 2003). Intense cycling of DON would affect the δ^{15}N-TDN, as shown by Schlarbaum et al. (2011) who found variation of more than 10 ‰ due to release and uptake of DON in a temperate estuary. Compensating N isotopic fractionation, e.g. from concomitant release, uptake, and degradation along the main channel resulting in a constant δ^{15}N-TDN cannot be excluded completely, but is considered unlikely (Knapp et al., 2005). Bioavailable DON produced in the reservoir might rapidly be degraded or taken up by bacteria or phytoplankton before reaching the Kafue Flats (Bronk et al., 1994).

BGD
9, 7943–7981, 2012

While δ^{15}N-TDN remained fairly constant along the Kafue River, δ^{15}N-PON decreased by >2‰ in the flooding season (Fig. 4), most likely due to the lateral input or in-situ production of PON with lower δ^{15}N. The fixation of atmospheric N leads to a δ^{15}N close to 0‰ in the fixed product (Martinelli et al., 1992) and the observed ^{15}N-depleted PON could thus be dominated by N-fixing organisms. Previous studies in tropical floodplains have found N-fixation rates of several g N m^{-2} yr^{-1} (Cleveland et al., 1999), through symbiotic (Martinelli et al., 1992) or through asymbiotic fixation by free-floating or attached cyanobacteria (Kern and Darwich, 2003). To balance the overall N budget N-fixation rates that high but comparable with measured rates in other systems would be needed. This is consistent with the isotope mass balance which requires a mean δ^{15}N of 1.0‰ and supports the hypothesis that N-fixation is the main N source to the Kafue Flats (Fig. 9b). The high abundance of periphyton on inundated vegetation and the high diversity and spreading of N-fixing plants in the floodplain (Ellenbroek, 1987) support this idea. The complementary measurements of N pools across the Kafue Flats fell in a relatively narrow range (–1 to 4‰; Table S1, supplement), which is within the data range reported for the Amazon floodplains (Aufdenkampe et al., 2007; Hedges et al., 2000; Bernardes et al., 2004) and may be characteristic for such systems.

5 Conclusions

During the flooding season, up to 80 % of the discharge in the Kafue River passed through the floodplain. This intense river-floodplain exchange caused net exports of 35–75 kg C km^{-2} d^{-1} in the form of DOC, which exceeded specific export rates predicted for the Amazon or the Congo River basins by a factor of 5 or more (5–14 kg C km^{-2} d^{-1}; Harrison et al., 2005; Mayorga et al., 2010). Stable isotope and spectroscopic analyses showed that DOM was mainly of terrestrial origin, but devoid of any distinct plant-derived signal. Export of authochtonous DOM from the upstream reservoir thus seems to be of minor importance. The exported POM was clearly

BGD
9, 7943–7981, 2012

distinguishable from DOM by its overall lower C:N ratio and lower $\delta^{13}C$. Both indicators underline the phytoplankton origin of POM. In the upper parts of the Kafue Flats, the POM pool was dominated by algal OM from the reservoir, and, further downstream, by phytoplankton or periphyton production in the floodplain based on a OC and ON mass balance.

The Kafue Flats are a net source of N to downstream ecosystems, despite a 50 % removal of riverine N by the upstream dam. A N mass and isotopic balance suggest that high N-fixation rates are needed to compensate the annual deficit of 21 000 t N. Our study underlines how intense river-floodplain exchange leads to very high OM export to a tropical river basin. In contrast to a forested system like the Amazon, the flooded grassland ecosystem of the Kafue Flats exports more phytoplankton POM than plant debris. Finally, the upstream reservoir had little effect on overall DOM quality, which indicates that aquatic DOM production in the reservoir was negligible compared to the large wetland sources.

Supplementary material related to this article is available online at: http://www.biogeosciences-discuss.net/9/7943/2012/bgd-9-7943-2012-supplement.pdf.

Acknowledgements. The authors thank Jason Wamulume, Griffin Shanungu, Manuel Kunz, Wilma Blaser, and Event Ngandu and the ZAWA wildlife officers for assistance during field work; Mark Rollog (University of Basel), Ruth Stierli (Eawag), Kate Ashe, the ETHZ Soil Chemistry and Environmental Chemistry groups for laboratory support, Britt Peterson (ETHZ) for assistance with excitation-emission spectroscopy analyses, Linda Jørgensen (University of Copenhagen) and Dolly Kothawala (University of Uppsala) for support with PARAFAC modeling and interpretation. This study was supported by the following Zambian partners and agencies: Imasiku Nyambe (University of Zambia), Zambia Wildlife Authority, Zambia Electricity Supply Corporation (ZESCO), Zambezi River Authority, and the Department of Water Affairs. Funding was provided by the Competence Center for Environment and Sustainability (CCES) of the ETH domain, the Swiss National Science Foundation (Grant No. 128707) and Eawag.

BGD
9, 7943–7981, 2012

References

Aalto, R., Maurice-Bourgoin, L., Dunne, T., Montgomery, D. R., Nittrouer, C. A., and Guyot, J. L.: Episodic sediment accumulation on Amazonian flood plains influenced by El Niño/Southern Oscillation, Nature, 425, 493–497, doi:10.1038/nature02002, 2003.

Alin, S. R., Aalto, R., Goni, M. A., Richey, J. E., and Dietrich, W. E.: Biogeochemical characterization of carbon sources in the strickland and fly rivers, Papua New Guinea, J. Geophys. Res.-Earth, 113, doi:05 10.1029/2006jf000625, 2008.

Aufdenkampe, A. K., Mayorga, E., Hedges, J. I., Llerena, C., Quay, P. D., Gudeman, J., Krusche, A. V., and Richey, J. E.: Organic matter in the Peruvian headwaters of the Amazon: Compositional evolution from the Andes to the lowland Amazon mainstem, Org. Geochem., 38, 337–364, doi:10.1016/j.orggeochem.2006.06.003, 2007.

Bastviken, D., Santoro, A. L., Marotta, H., Pinho, L. Q., Calheiros, D. F., Crill, P., and Enrich-Prast, A.: Methane Emissions from Pantanal, South America, during the Low Water Season: Toward More Comprehensive Sampling, Environ. Sci. Technol., 44, 5450–5455, doi:10.1021/es1005048, 2010.

Battin, T. J., Luyssaert, S., Kaplan, L. A., Aufdenkampe, A. K., Richter, A., and Tranvik, L. J.: The boundless carbon cycle, Nat. Geosci., 2, 598–600, doi:10.1038/ngeo618, 2009.

Berman, T. and Bronk, D. A.: Dissolved organic nitrogen: a dynamic participant in aquatic ecosystems, Aquat. Microb. Ecol., 31, 279–305, 2003.

Bernardes, M. C., Martinelli, L. A., Krusche, A. V., Gudeman, J., Moreira, M., Victoria, R. L., Ometto, J., Ballester, M. V. R., Aufdenkampe, A. K., Richey, J. E., and Hedges, J. I.: Riverine organic matter composition as a function of land use changes, Southwest Amazon, Ecol. Appl., 14, 263–279, 2004.

Bouillon, S., Dehairs, F., Schiettecatte, L. S., and Borges, A. V.: Biogeochemistry of the Tana estuary and delta (Northern Kenya), Limnol. Oceanogr., 52, 46–59, 2007.

Bouillon, S., Abril, G., Borges, A. V., Dehairs, F., Govers, G., Hughes, H. J., Merckx, R., Meysman, F. J. R., Nyunja, J., Osburn, C., and Middelburg, J. J.: Distribution, origin and cycling of carbon in the Tana River (Kenya): a dry season basin-scale survey from headwaters to the delta, Biogeosciences, 6, 2475–2493, doi:10.5194/bg-6-2475-2009, 2009.

Bourbonnais, A., Lehmann, M. F., Waniek, J. J., and Schulz-Bull, D. E.: Nitrate isotope anomalies reflect N_2 fixation in the Azores Front region (subtropical NE Atlantic), J. Geophys. Res.-Oceans, 114, doi:10.1029/2007jc004617, 2009.

BGD
9, 7943–7981, 2012

Braman, R. S. and Hendrix, S. A.: Nanogram nitrite and nitrate determination in environmental and biological materials by vanadium(III) reduction with chemiluminescence detection, Anal. Chem., 61, 2715–2718, 1989.
Bronk, D. A., Glibert, P. M., and Ward, B. B.: Nitrogen uptake, dissolved organic nitrogen release, and new production, Science, 265, 1843–1846, 1994.
Bronk, D. A., Lomas, M. W., Glibert, P. M., Schukert, K. J., and Sanderson, M. P.: Total dissolved nitrogen analysis: comparisons between the persulfate, UV and high temperature oxidation methods, Mar. Chem., 69, 163–178, 2000.
Casciotti, K. L., Sigman, D. M., Hastings, M. G., Böhlke, J. K., and Hilkert, A.: Measurement of the oxygen isotopic composition of nitrate in seawater and freshwater using the denitrifier method, Anal. Chem., 74, 4905–4912, 2002.
Chen, F. J. and Jia, G. D.: Spatial and seasonal variations in δ^{13}C and δ^{15}N of particulate organic matter in a dam-controlled subtropical river, River Res. Appl., 25, 1169–1176, doi:10.1002/rra.1225, 2009.
Chen, H. and Zheng, B. H.: Characterizing natural dissolved organic matter in a freshly submerged catchment (Three Gorges Dam, China) using UV absorption, fluorescence spectroscopy and PARAFAC, Water Sci. Technol., 65, 962–969, doi:10.2166/wst.2012.939, 2012.
Chen, W., Westerhoff, P., Leenheer, J. A., and Booksh, K.: Fluorescence excitation – Emission matrix regional integration to quantify spectra for dissolved organic matter, Environ. Sci. Technol., 37, 5701–5710, doi:10.1021/es034354c, 2003.
Cleveland, C. C., Townsend, A. R., Schimel, D. S., Fisher, H., Howarth, R. W., Hedin, L. O., Perakis, S. S., Latty, E. F., Von Fischer, J. C., Elseroad, A., and Wasson, M. F.: Global patterns of terrestrial biological nitrogen (N_2) fixation in natural ecosystems, Global Biogeochem. Cy., 13, 623–645, doi:10.1029/1999gb900014, 1999.
Coble, P. G.: Characterization of marine and terrestrial DOM in seawater using excitation emission matrix spectroscopy, Mar. Chem., 51, 325–346, 1996.
Cory, R. M. and McKnight, D. M.: Fluorescence spectroscopy reveals ubiquitous presence of oxidized and reduced quinones in dissolved organic matter, Environ. Sci. Technol., 39, 8142–8149, doi:10.1021/es0506962, 2005.
Cory, R. M., Miller, M. P., McKnight, D. M., Guerard, J. J., and Miller, P. L.: Effect of instrument-specific response on the analysis of fulvic acid fluorescence spectra, Limnol. Oceanogr-Methods, 8, 67–78, 2010.

BGD
9, 7943–7981, 2012

Cotner, J. B., Montoya, J. V., Roelke, D. L., and Winemiller, K. O.: Seasonally variable riverine production in the Venezuelan llanos, J. N. Am. Benthol. Soc., 25, 171–184, doi:10.1899/0887-3593(2006)25[171:SVRIPIT]2.0.CO;2, 2006.
Ellenbroek, G. A.: Ecology and Productivity of an African Wetland System, Geobotany 9, edited by: Junk, Dr, W., Dordrecht, 1987.
Gergel, S. E., Carpenter, S. R., and Stanley, E. H.: Do dams and levees impact nitrogen cycling? Simulating the effects of flood alterations on floodplain denitrification, Glob. Change Biol., 11, 1352–1367, 2005.
Grasshoff, K., Kremling, K., and Ehrhardt, M.: Methods of Seawater Analysis, 3rd ed., Wiley-VCH, Weinheim, New York, Chichester Brisbane, Singapore, Tokyo, 632 pp., 1999.
Hamilton, S. K. and Lewis, W. M.: Stable carbon and nitrogen isotopes in algae and detritus from the Orinoco River floodplain, Venezuela, Geochim. Cosmochim. Ac., 56, 4237–4246, 1992.
Harrison, J. A., Caraco, N., and Seitzinger, S. P.: Global patterns and sources of dissolved organic matter export to the coastal zone: Results from a spatially explicit, global model, Global Biogeochem. Cy., 19, doi:10.1029/2005gb002480, 2005.
Hedges, J. I., Mayorga, E., Tsamakis, E., McClain, M. E., Aufdenkampe, A., Quay, P., Richey, J. E., Benner, R., Opsahl, S., Black, B., Pimentel, T., Quintanilla, J., and Maurice, L.: Organic matter in Bolivian tributaries of the Amazon River: A comparison to the lower mainstream, Limnol. Oceanogr., 45, 1449–1466, 2000.
Hunsinger, G. B., Mitra, S., Findlay, S. E. G., and Fischer, D. T.: Wetland-driven shifts in suspended particulate organic matter composition of the Hudson River estuary, New York, Limnol. Oceanogr., 55, 1653–1667, 2010.
Ishii, S. K. L. and Boyer, T. H.: Behavior of reoccurring PARAFAC components in fluorescent dissolved organic matter in natural and engineered systems: a critical review, Environ. Sci. Technol., 46, 2006–2017, doi:10.1021/es2043504, 2012.
Johnson, M. S., Couto, E. G., Abdo, M., and Lehmann, J.: Fluorescence index as an indicator of dissolved organic carbon quality in hydrologic flowpaths of forested tropical watersheds, Biogeochemistry, 105, 149–157, doi:10.1007/s10533-011-9595-x, 2011.
Kern, J., Darwich, A., Furch, K., and Junk, W. J.: Seasonal denitrification in flooded and exposed sediments from the Amazon floodplain at Lago Camaleão, Microb. Ecol., 32, 47–57, 1996.
Kern, J. and Darwich, A.: The role of periphytic N_2 fixation for stands of macrophytes in the whitewater floodplain (varzea), Amazoniana, 17, 361–375, 2003.

BGD
9, 7943–7981, 2012

Knapp, A. N., Sigman, D. M., and Lipschultz, F.: N isotopic composition of dissolved organic nitrogen and nitrate at the Bermuda Atlantic time-series study site, Global Biogeochem. Cy., 19, doi:10.1029/2004gb002320, 2005.
Kunz, M. J., Wüest, A., Wehrli, B., Landert, J., and Senn, D. B.: Impact of a large tropical reservoir on riverine transport of sediment, carbon, and nutrients to downstream wetlands, Water Resour. Res., 47, 16, doi:10.1029/2011WR010996, 2011.
Lakowicz, J. R.: Principles of Fluorescence Spectroscopy, 3rd ed., Springer, New York, 954 pp., 2006.
Ludwig, W., Probst, J. L., and Kempe, S.: Predicting the oceanic input of organic carbon by continental erosion, Global Biogeochem. Cy., 10, 23–41, doi:10.1029/95gb02925, 1996.
Maie, N., Jaffé, R., Miyoshi, T., and Childers, D. L.: Quantitative and qualitative aspects of dissolved organic carbon leached from senescent plants in an oligotrophic wetland, Biogeochemistry, 78, 285–314, doi:10.1007/s10533-005-4329-6, 2006.
Martinelli, L. A., Victoria, R. L., Trivelin, P. C. O., Devol, A. H., and Richey, J. E.: N-15 natural abundance in plants of the Amazon River floodplain and potential atmospheric N_2 fixation, Oecologia, 90, 591–596, 1992.
Mayorga, E., Aufdenkampe, A. K., Masiello, C. A., Krusche, A. V., Hedges, J. I., Quay, P. D., Richey, J. E., and Brown, T. A.: Young organic matter as a source of carbon dioxide outgassing from Amazonian rivers, Nature, 436, 538–541, doi:10.1038/nature03880, 2005.
Mayorga, E., Seitzinger, S. P., Harrison, J. A., Dumont, E., Beusen, A. H. W., Bouwman, A. F., Fekete, B. M., Kroeze, C., and Van Drecht, G.: Global nutrient export from WaterSheds 2 (NEWS 2): model development and implementation, Environ. Modell. Softw., 25, 837–853, doi:10.1016/j.envsoft.2010.01.007, 2010.
McKnight, D. M., Boyer, E. W., Westerhoff, P. K., Doran, P. T., Kulbe, T., and Andersen, D. T.: Spectrofluorometric characterization of dissolved organic matter for indication of precursor organic material and aromaticity, Limnol. Oceanogr., 46, 38–48, 2001.
Meier, P., Wang, H., Milzow, C., and Kinzelbach, W.: Remote sensing for hydrological modeling of seasonal wetlands – concepts and applications, ESA Living Planet Symposium, 28 June–2 July 2010, Bergen, Norway, 2010.
Mladenov, N., McKnight, D. M., Wolski, P., and Ramberg, L.: Effects of annual flooding on dissolved organic carbon dynamics within a pristine wetland, the Okavango Delta, Botswana, Wetlands, 25, 622–638, 2005.

BGD
9, 7943–7981, 2012

Mumba, M. and Thompson, J. R.: Hydrological and ecological impacts of dams on the Kafue Flats floodplain system, Southern Zambia, Phys. Chem. Earth, 30, 442–447, 2005.
Munyati, C.: Wetland change detection on the Kafue Flats, Zambia, by classification of a multitemporal remote sensing image dataset, Int. J. Remote Sens., 21, 1787–1806, 2000.
Petrone, K. C., Fellman, J. B., Hood, E., Donn, M. J., and Grierson, P. F.: The origin and function of dissolved organic matter in agro-urban coastal streams, J. Geophys. Res.-Biogeosciences, 116, 13, doi:10.1029/2010jg001537, 2011.
Raymond, P. A. and Bauer, J. E.: Riverine export of aged terrestrial organic matter to the North Atlantic Ocean, Nature, 409, 497–500, 2001.
Richey, J. E., Mertes, L. A. K., Dunne, T., Victoria, R. L., Forsberg, B. R., Tancredi, A. C. N. S., and Oliveira, E.: Sources and routing of the Amazon River flood wave, Global Biogeochem. Cy., 3, 191–204, 1989.
Richey, J. E., Hedges, J. I., Devol, A. H., Quay, P. D., Victoria, R., Martinelli, L., and Forsberg, B. R.: Biogeochemistry of carbon in the Amazon River, Limnol. Oceanogr., 35, 352–371, 1990.
Schlarbaum, T., Dähnke, K., and Emeis, K.: Dissolved and particulate reactive nitrogen in the Elbe River/NW Europe: a 2-yr N-isotope study, Biogeosciences, 8, 3519–3530, doi:10.5194/bg-8-3519-2011, 2011.
Schwendenmann, L. and Veldkamp, E.: The role of dissolved organic carbon, dissolved organic nitrogen, and dissolved inorganic nitrogen in a tropical wet forest ecosystem, Ecosystems, 8, 339–351, doi:10.1007/s10021-003-0088-1, 2005.
Sigman, D. M., Casciotti, K. L., Andreani, M., Barford, C., Galanter, M., and Böhlke, J. K.: A bacterial method for the nitrogen isotopic analysis of nitrate in seawater and freshwater, Anal. Chem., 73, 4145–4153, 2001.
Solorzano, L. and Sharp, J. H.: Determination of total dissolved nitrogen in natural waters, Limnol. Oceanogr., 25, 751–754, 1980.
Spencer, R. G. M., Hernes, P. J., Ruf, R., Baker, A., Dyda, R. Y., Stubbins, A., and Six, J.: Temporal controls on dissolved organic matter and lignin biogeochemistry in a pristine tropical river, Democratic Republic of Congo, J. Geophys. Res.-Biogeosciences, 115, doi:10.1029/2009jg001180, 2010.
Stedmon, C. A. and Bro, R.: Characterizing dissolved organic matter fluorescence with parallel factor analysis: a tutorial, Limnol. Oceanogr.-Methods, 6, 572–579, 2008.

BGD
9, 7943–7981, 2012

Stedmon, C. A. and Markager, S.: Resolving the variability in dissolved organic matter fluorescence in a temperate estuary and its catchment using PARAFAC analysis, Limnol. Oceanogr., 50, 686–697, 2005.
Stedmon, C. A., Markager, S., and Bro, R.: Tracing dissolved organic matter in aquatic environments using a new approach to fluorescence spectroscopy, Mar. Chem., 82, 239–254, doi:10.1016/s0304-4203(03)00072-0, 2003.
Tremblay, L. and Benner, R.: Organic matter diagenesis and bacterial contributions to detrital carbon and nitrogen in the Amazon River system, Limnol. Oceanogr., 54, 681–691, 2009.
Villar, C. A., de Cabo, L., Vaithiyanathan, P., and Bonetto, C.: River-floodplain interactions: nutrient concentrations in the Lower Parana River, Arch. Hydrobiol., 142, 433–450, 1998.
Vörösmarty, C. J., Meybeck, M., Fekete, B., Sharma, K., Green, P., and Syvitski, J. P. M.: Anthropogenic sediment retention: major global impact from registered river impoundments, Global Planet. Change, 39, 169–190, doi:10.1016/s0921-8181(03)00023-7, 2003.
Wamulume, J., Landert, J., Zurbrügg, R., Nyambe, I., Wehrli, B., and Senn, D. B.: Exploring the hydrology and biogeochemistry of the dam-impacted Kafue River and Kafue Flats (Zambia), Phys. Chem. Earth, 36, 775–788, doi:10.1016/j.pce.2011.07.049, 2011.
Weishaar, J. L., Aiken, G. R., Bergamaschi, B. A., Fram, M. S., Fujii, R., and Mopper, K.: Evaluation of specific ultraviolet absorbance as an indicator of the chemical composition and reactivity of dissolved organic carbon, Environ. Sci. Technol., 37, 4702-4708, doi:10.1021/es030360x, 2003.
Wiegner, T. N., Tubal, R. L., and MacKenzie, R. A.: Bioavailability and export of dissolved organic matter from a tropical river during base- and stormflow conditions, Limnol. Oceanogr., 54, 1233–1242, doi:10.4319/lo.2009.54.4.1233, 2009.
Yamashita, Y., Maie, N., Briceno, H., and Jaffé, R.: Optical characterization of dissolved organic matter in tropical rivers of the Guayana Shield, Venezuela, J. Geophys. Res.-Biogeosciences, 115, doi:10.1029/2009jg000987, 2010a.
Yamashita, Y., Scinto, L. J., Maie, N., and Jaffé, R.: Dissolved organic matter characteristics across a subtropical wetland's landscape: application of optical properties in the assessment of environmental dynamics, Ecosystems, 13, 1006–1019, doi:10.1007/s10021-010-9370-1, 2010b.
Ziegler, S. E. and Brisco, S. L.: Relationships between the isotopic composition of dissolved organic carbon and its bioavailability in contrasting Ozark streams, Hydrobiologia, 513, 153–169, doi:10.1023/B:hydr.0000018180.54292.47, 2004.

BGD
9, 7943–7981, 2012

Zurbrügg, R., Wamulume, J., Kamanga, R., Wehrli, B., and Senn, D. B.: River-floodplain exchange and its effects on the fluvial oxygen regime in a large tropical river system (Kafue Flats, Zambia), J. Geophys. Res.-Biogeosciences, in press, 2012.

BGD
9, 7943–7981, 2012

Table 1. Organic carbon and nitrogen loads, net exports and yields from the Kafue Flats.

	Export from Kafue Flats[a] (t C or N d^{-1})	Load increase after ~230 km[b] (×)	Floodplain contribution to export[c] (%)	Net export[d] (t C or N d^{-1})	Yields (kg C or N km^{-2} d^{-1})[e]
May 2010 – flooding season					
DOC	339	3.3	82	214	69.8
POC	35.7	3.0	92	14.9	4.9
DON	13.6	4.6	75	7.6	2.5
PON	5.1	11	88	1.4	0.5
DIN	1.6	7.6	85	0.6	0.2
May 2009 – flooding season					
DOC	210	2.5	72	108	35.2
POC	15.6	4.0	80	–0.2	–0.1
DON	11.5	3.0	75	6.0	2.0
PON	2.0	3.5	78	0.0	0.0
DIN	0.9	4.1	80	–0.2	–0.1
Oct 2008 – dry season					
DOC	48.1	n.a.	n.a.	–6.9	n.a.
POC	7.4	n.a.	n.a.	–9.3	n.a.
DON	2.9	n.a.	n.a.	–0.5	n.a.
PON	0.9	n.a.	n.a.	–0.7	n.a.
DIN	0.1	n.a.	n.a.	–0.2	n.a.

[a] Calculated as discharge × concentration at the outflow (410 km).

[b] Flooding season C and N loads had a minimum at ~230 km, caused by a channel constriction and reduced river discharge (marked with arrow in Fig. 7). The increase in C and N loads thereafter were assumed to originate from the floodplain.

[c] The floodplain contribution to the exported OM was calculated under the assumption of negligible in-stream production of DOM or POM.

[d] Calculated as the difference of discharge × concentration between 0 km and 410 km.

[e] The export per area was calculated using the maximum flooded area for the rainy season 2009/2010 of 3060 km^2 (Meier et al., 2010).

BGD
9, 7943–7981, 2012

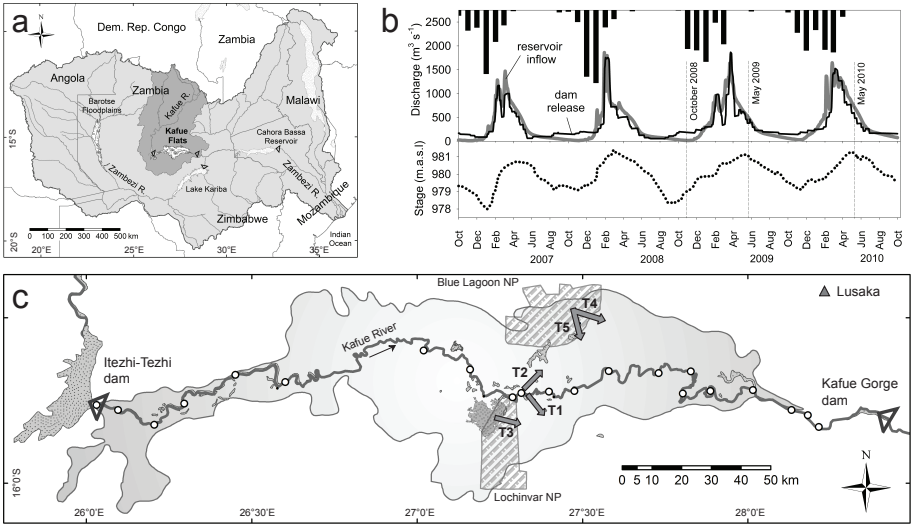

Fig. 1. (a) Kafue Flats in the Kafue River basin (dark shaded), a subbasin of the Zambezi River basin (light gray). **(b)** The hydrograph from 2007–2010 shows the reservoir inflow (gray line), dam release (black line), rainfall (bars), and to the water level in the middle of the floodplain (dotted line, lower panel). The three sampling campaigns are marked by vertical lines. **(c)** Map of the Kafue Flats. Large dams are marked with triangles, white dots indicate sampling stations along the main channel, arrows T1–T5 depict transects into the floodplain.

BGD
9, 7943–7981, 2012

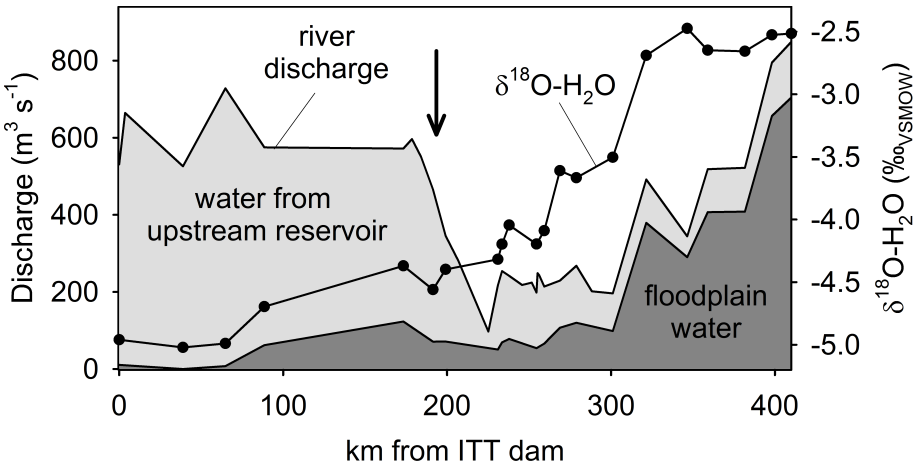

Fig. 2. Evidence of river-floodplain exchange in May 2010, indicated by an increasing proportion of floodplain-derived water (dark gray shading) relative to water discharged from the reservoir (light gray shading). The contribution of floodplain water was calculated by a mixing model based on δ^{18}O-H_2O along the river (full circles). For details see Zurbrügg et al. (2012). The arrow marks the steep decline in discharge (180–225 km) caused by a constriction in the river channel.

BGD
9, 7943–7981, 2012

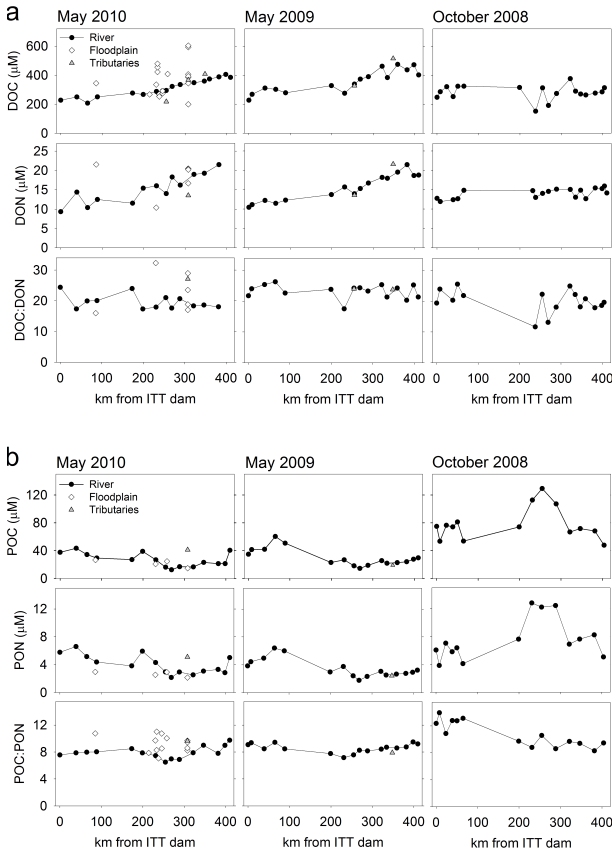

Fig. 3. (a) Concentrations of DOC and DON, and molar DOC:DON ratio, **(b)** concentrations of POC and PON, and molar POC:PON ratio for May 2010, May 2009, and October 2008 along the Kafue River channel (black dots and lines), at floodplain stations (empty diamonds) and tributaries (gray triangles).

BGD
9, 7943–7981, 2012

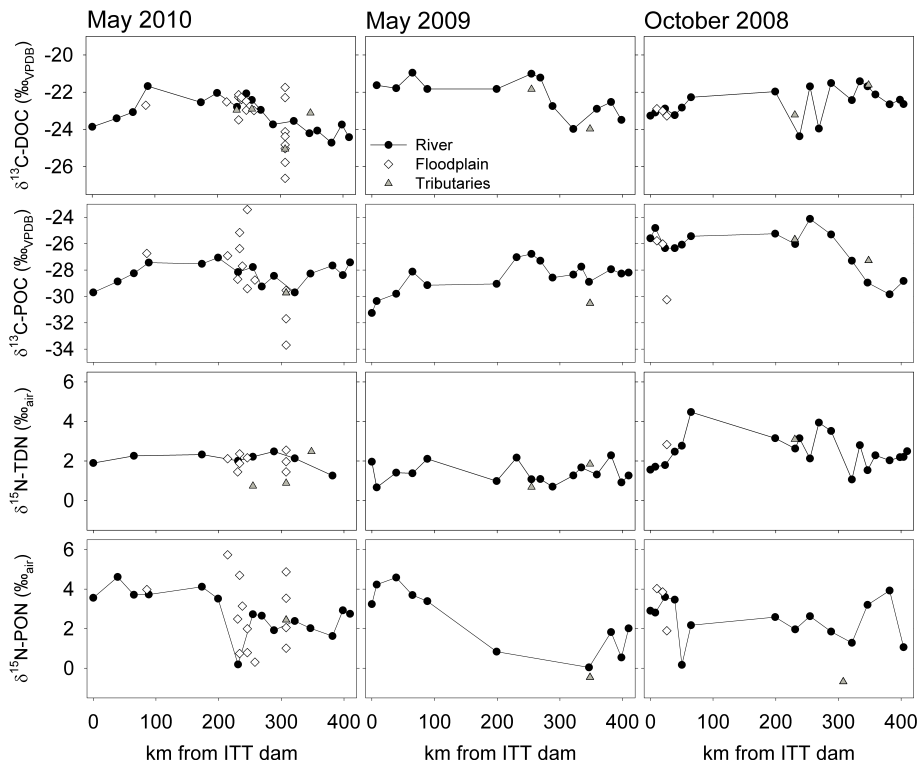

Fig. 4. Stable isotope signatures of dissolved and particulate organic carbon and nitrogen for the three sampling campaigns (symbols as indicated in Fig. 3).

BGD
9, 7943–7981, 2012

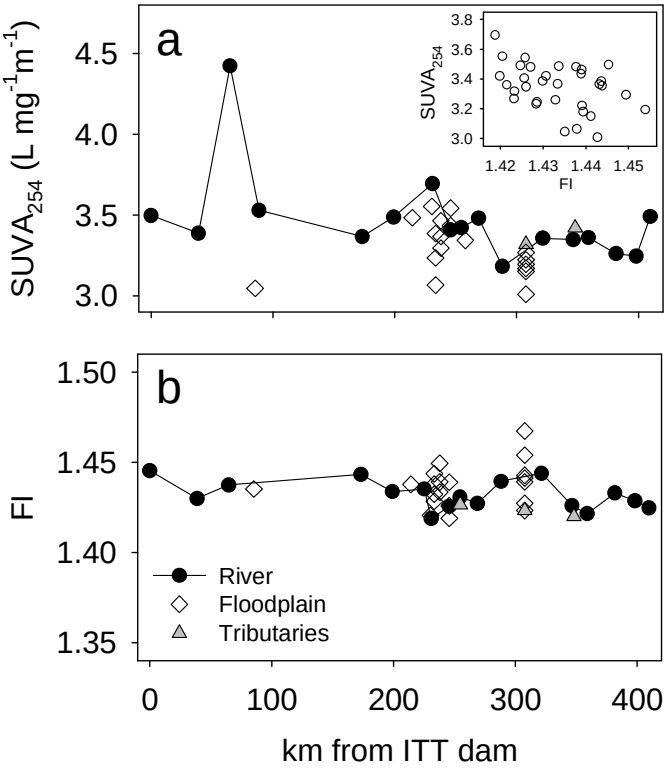

Fig. 5. (a) Specific UV absorption at 254 nm ($SUVA_{254}$), and **(b)** fluorescence index (FI) along the river (black circles) and the in floodplain (empty diamonds) and in tributaries (gray triangles) in May 2010. The inlaid in **(a)** shows the negative correlation of the pooled $SUVA_{254}$ and FI data ($P < 0.001$). Samples with $SUVA_{254} > 4.0\,l\,mg^{-1}\,m^{-1}$ were removed for clarity.

BGD
9, 7943–7981, 2012

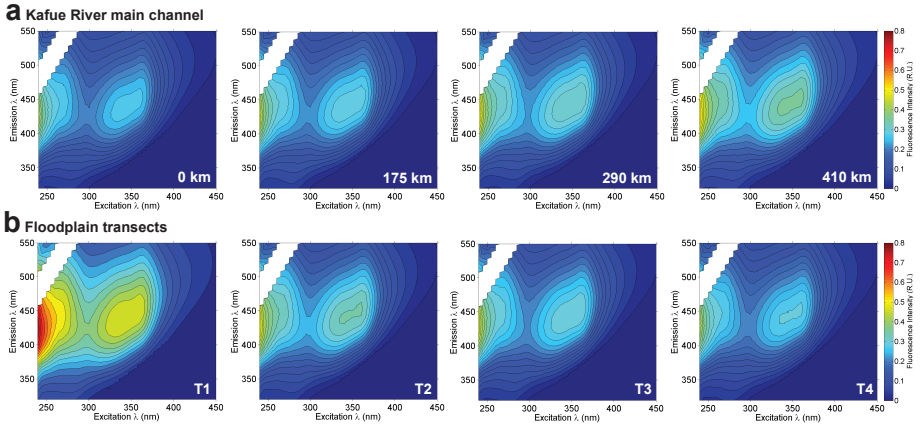

Fig. 6. Excitation-emission matrices (EEMs) for **(a)** four river samples indicated with distance from ITT dam, and **(b)** four floodplain samples on different floodplain transects. The two main fluorescence peaks are at excitation/emission wavelengths of 240/430 nm and 345/440 nm, and have been named by Coble (1996) as Peak A and Peak C, respectively.

BGD
9, 7943–7981, 2012

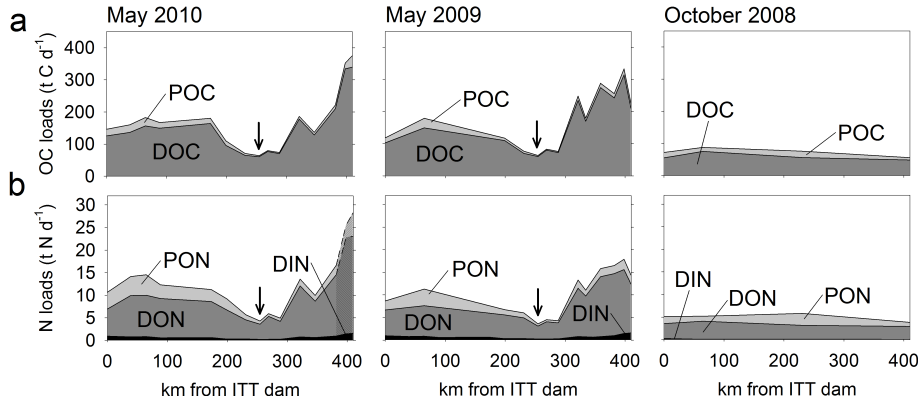

Fig. 7. (a) Organic carbon loads (t C d^{-1}) and **(b)** organic nitrogen loads (t N d^{-1}) calculated as discharge × concentration for the three sampling campaigns. The hatched areas in May 2010 N loads are calculated with concentrations extrapolated from the regression line between DOC and DON ($\rho = 0.901$, $P < 0.001$), due to missing DON data. Arrows indicate the discharge minimum due to a channel constriction from Zurbrügg et al. (2012).

BGD
9, 7943–7981, 2012

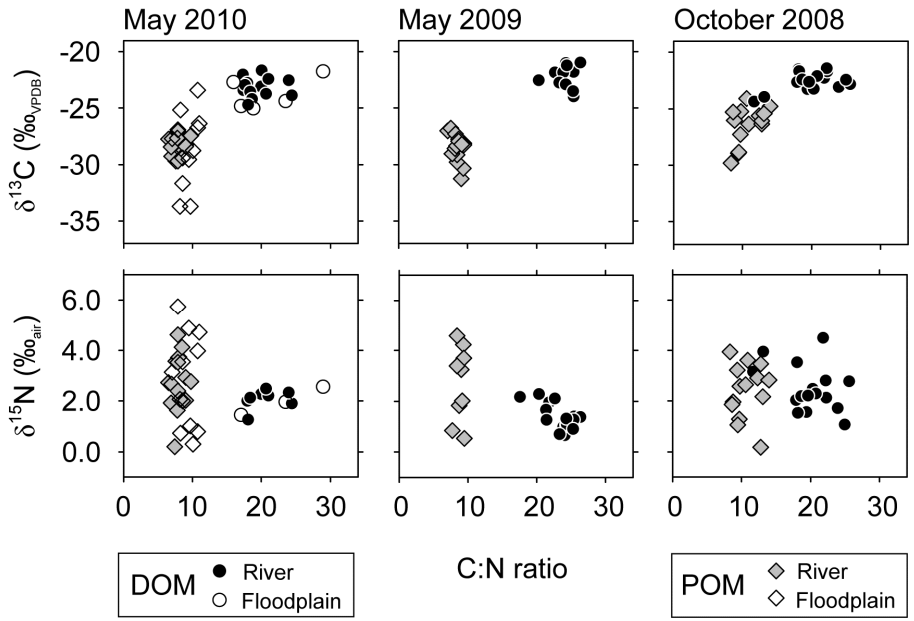

Fig. 8. δ^{13}C and δ^{15}N values of dissolved and particulate organic matter, relative to their C:N ratio. Significant differences ($P < 0.05$) were found between C:N ratios and δ^{13}C of DOM and POM, throughout all sampling campaigns, but not for δ^{15}N.

BGD
9, 7943–7981, 2012

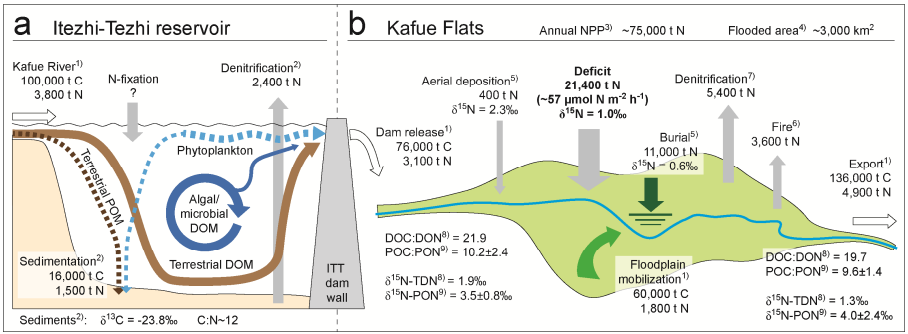

Fig. 9. (a) Schematic illustration of the annual C and N fluxes in ITT reservoir. **(b)** System-scale N balance of the Kafue Flats based on own data and literature estimations. [1)] data from Wamulume et al. (2011); [2)] data from Kunz et al. (2011); [3)] estimated based on Ellenbroek (1987); [4)] from the model of Meier et al. (2010); [5)] Deposition based on trap data, burial from on sediment cores (R. Zurbrügg, unpublished data); [6)] burnt areas from Munyati (2000); [7)] Estimated based on studies from the Amazon floodplains (Kern et al., 1996); [8)] data from October 2008, May 2009, and May 2010; [9)] data from annual sampling campaign (Fig. S3, supplement).

BGD
9, 7943–7981, 2012

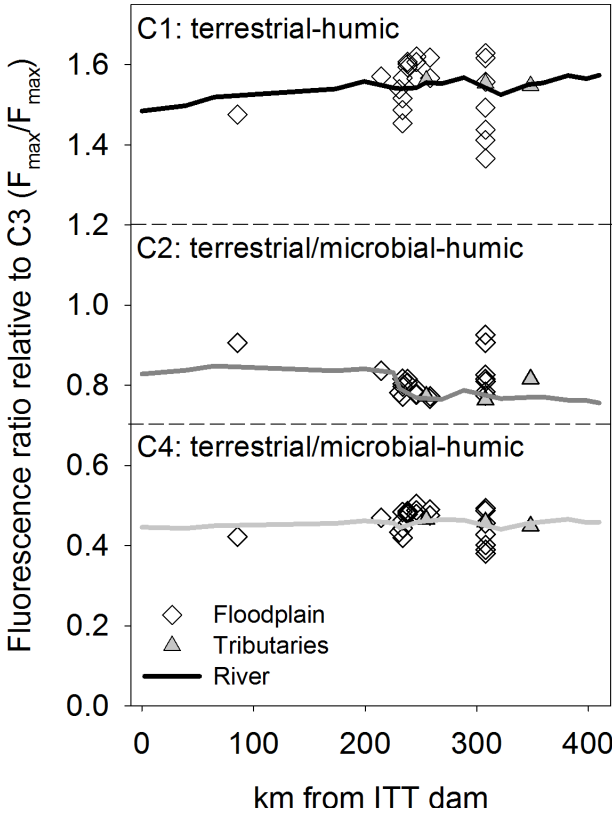

Fig. 10. Ratios of components, identified by PARAFAC analysis. Components C1, C2, and C4 are shown relative to C3 along the river, in floodplain and tributaries, measured in May 2010.

BGD
9, 7943–7981, 2012